

Experimental study of water-oil-boom interaction and failure events

D. Borri¹ C. Lugni^{1,2} M. Greco^{1,2} O.M. Faltinsen¹
daniele.borri@ntnu.no claudio.lugni@cnr.it marilena.greco@ntnu.no odd.faltinsen@ntnu.no

1 Centre for Autonomous Marine Operations and Systems (AMOS),
Department of Marine Technology, NTNU, Trondheim – Norway.
2 CNR-INSEAN, Italian Ship Model Basin, Roma – Italy.

Oil spill caused by maritime accidents can damage valuable ecosystems and have a huge economic impact on fishing and tourism industries. In order to minimize the damage it is important to predict the trajectory of the spilled oil slick and use an effective clean-up strategy. Oil booms represent a valid solution, but their performance has a limitation in sufficiently strong currents and high sea waves. This motivated research efforts in the development of suitable prediction tools useful for the design and for setting the operative limits of these devices. Experiments are instead more difficult to perform. However some relevant studies have been documented along the years, most of them in 2D conditions, with fixed boom and in steady current. For example, Delvigne (1989) studied a scaled boom interacting with different types of oil and identified the failure mechanisms involved. A comprehensive documentation of full- and model-scale tests in 2D and 3D conditions is provided *e.g.* by Grilli *et al.* (2000).

Here a physical investigation is ongoing based on dedicated model tests to be used for gaining further insights on the phenomena involved and as reference data for numerical-tools development. The experimental set-up and some of the results of the analysis are discussed in the following.

Experimental set-up The model tests were performed inside a tank with internal length, height and width, respectively, $L = 3$ m, $H = 0.6$ m and $w = 0.1$ m, at the CNR-INSEAN Sloshing Lab. The experimental set-up is shown in the left of figure 1 and was designed for 2D flow conditions in the tank. However clear 3D features were recorded when instabilities and boom failures occurred. The tank is made of perspex sheets, 1.5 cm thick, and is fixed at the edges to an aluminum



Figure 1: Left: tank mounted on the 6-DOF MISTRAL Hexapode excitation mechanism. Right: boom model and pressure sensors.

frame for structural strengthening. Vertical reinforcements along the front and rear walls were not used in order to have an optimal view of the flow. The boom, in scale 1:6, is shown in the right of the figure. It is realized in rigid expanded polyurethane but geometrically reproducing the different parts of a real boom with an outer floater radius $r_{out} = 4$ cm, a draft $D = 11$ cm and a skirt height $h_{skirt} = 8$ cm. It was equipped with seven pressure sensors with sampling frequency 10kHz: two transversally on the edge of the skirt and the others along the centerline of the cylinder, three on the oil side and two on the water side. The tank was filled of water up to 45 cm ($H_w = 0.75H$), so to ensure a ratio H_w/D sufficiently large, and therefore limited bottom effects on the phenomena, and to avoid liquid leakage from the tank (tested without roof). This arrangement was mounted on a 6-DOF motion simulator which prescribes a sway motion with steady-state amplitude of 0.15 m and frequency 0.2 Hz, after a ramp lasting for the first three periods. An accelerometer was used to check the quality of the enforced motion (see left plot of figure 2). These motion parameters were selected in order to realize a slowly-varying current with horizontal speeds of the liquid around 0.2 m/s, which is in the range for boom failure for the chosen geometry and scale (Delvigne 1989). The model was located in the central tank section, where the highest

liquid velocities inside the tank are obtained and failure can occur more easily. In order to reproduce a behavior similar to that of an operative boom, the model is left free in heave by two vertical fishing lines that act as a rail. In particular, each one is fixed at the tank bottom by a spring, it is anchored to a metal plate above the tank and passes through a pipe in the boom. This setting allows also a limited motion in sway and a partial rotation of the boom, mainly due to the deformation of the springs.

A prescribed amount of vegetable oil is released on the right side of the tank relative to the boom and, before starting a test, it is waited until the emulsion has disappeared and calm conditions are achieved. After each test with boom failure, the oil passed on the left side of the tank is collected and brought back to the right side. The oil stuck to the tank wall is removed with a piece of cloth but is then lost, leading to a variation in the oil volume which is however very limited. The oil is a soybean oil with density $\rho_o = 919 \text{ kg/m}^3$ and kinematic viscosity $\nu_o = 56 \cdot 10^{-6} \text{ m}^2/\text{s}$, chosen because of its non toxicity and its properties close to those of a more realistic Bunker B (BB) oil for which entrainment-boom failure typically occurs. One must note that the given density and viscosity refer to nominal values, a more precise evaluation would require a direct measurement of the oil properties. To prevent the oil from passing between the model and the tank walls a felt strip has been attached to the boom sides. Moreover, a thin layer of insulating acetoxy silicone was spread on it to avoid oil absorption.

Video recordings of the experiments were done using two low-speed cameras (with 25 fps) to provide a global view of the test and two high-speed cameras (with 100 fps) to give a detailed view of the flow nearby the boom. The two low-speed cameras have a view overlapping so to allow the reconstruction of the overall tank view by image analysis. Similarly it is done for the two others for a wider view around the boom. Using the images from the enlarged views and glass particles with 1μ diameter as seeding, the liquid velocities were measured with the Particle Tracking Velocimetry (PTV) technique (Miozzi 2004). A dedicated light system was used to properly illuminate the particles. An example of predicted water velocities is given in the right of figure 2 showing a vortical structure shed from the boom bottom.

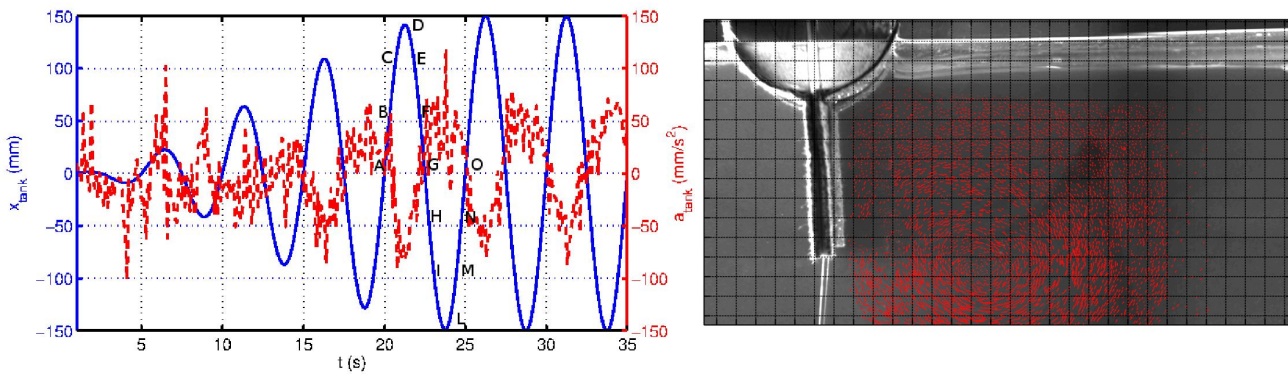


Figure 2: Right: prescribed sway motion (blue line) and measured acceleration (red line) of the tank. Left: enlarged view of the tank with the boom and the local velocities estimated with the PTV technique.

Preliminary standard sloshing tests, *i.e.* without boom and oil, were performed to characterize the flow and verify if velocities in the range of expected critical speed for the failure could be achieved in the central section of the tank. Then five different volumes of oil (V_0) were examined: 0.5, 0.7, 0.8, 0.9 and 11. In each case the oil was set on the right of the boom and tests until steady-state conditions were performed. The general features of the phenomena are discussed next in terms of the oil case with $V_0 = 11$.

General features The occurrence of boom failure is a possible consequence of an instability developing under certain conditions at the water-oil interface. The latter seems to be associated with the formation of a headwave (sloped interface leading to and including a thicker oil slick) when there is a combination of sufficiently large slope, thick slick and high local oil-water relative velocity. From a preliminary analysis of the present experimental data, the instability could be affected by the vortex shedding from the boom toward the oil side (see right panel of figure 2). Indeed the vortical structure seems to induce a minimum in the oil slick thickness in the first part of each motion period (*e.g.* from time instant A to about time instant D for the fifth period shown in the left plot of figure 2) contributing in the formation of a headwave close to the boom. However, when the instabilities originate at the oil-water interface the vortex is almost destroyed and can only affect the local inflow velocity in the later evolution. Let us consider a generic period with instability occurrence for $V_0 = 11$, *e.g.* the fifth period of the tank motion with labelled time instants in the left plot of figure 2. From A to B the oil headwave moves far from the boom. This process continues until D, when the tank position has reached its maximum. At this stage, a thickened area in the oil slick starts to form. After that the oil is pushed towards the boom and instabilities appear at the water-oil interface, in the form of growing waves traveling toward the boom. They

appear both in the mid section of the tank and along the front wall, with clear 3D features. This behavior is qualitatively similar for each period with instability. What happens later depends on the strength of the instability and on the kinematic flow conditions in the specific case. For the amount of oil here considered, the instability occurs the first time at the fourth period (see left plot of figure 3) but it is weak and disappears without consequences. At the fifth period it is able to lead

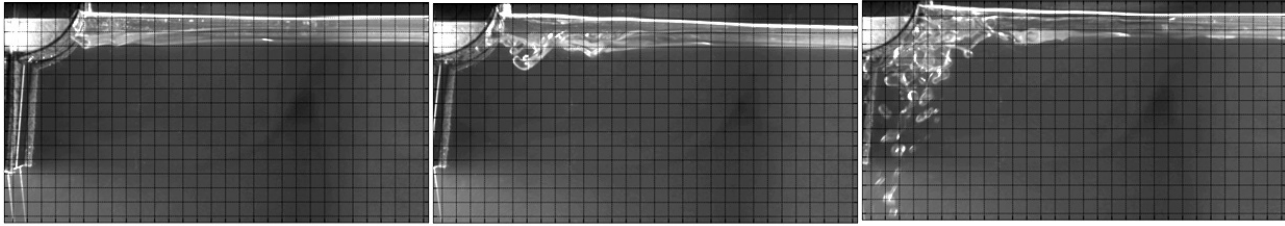


Figure 3: From left to right: enlarged views with instability of water-oil interface during the fourth, fifth and sixth period of the tank oscillation for the case with $V_0 = 11$. These instants are near the time G in the corresponding period (see left plot of figure 2 for G definition) and show the maximum amplitude of the instability for the fourth and fifth periods and the onset of boom failure for the sixth period.

to interface breaking with spilling of oil drops into water, but not to a boom failure (see centre plot of figure 3). The latter occurs at the sixth period because of a sufficiently high local speed (see right plot of figure 3) and is an entrainment failure with filaments and droplets of oil detaching from the oil slick and passing beneath the boom. For all three periods the instability starts between the corresponding time instants E and F , soon after the tank has started to move from the oil side toward the boom. The sixth period is in steady-state conditions for the tank motion (see left plot of figure 2), however also in the following periods the flow features close to the boom do not repeat periodically because part of the oil moves to the left side of the tank reducing the amount on the right. Similar conditions occur with the other amounts of oil.

The used experimental set-up allows only a rough estimate of the wavelengths, speed and growth rate of the instabilities. A closer view to these parameters would help in clarifying the nature of the instabilities. From our preliminary investigations they could start as Holmboe waves which become steep in time and may transform in Kelvin-Helmoltz instabilities if they are energetic enough. The latter seems to be the responsible for interface breaking with oil drops spilling in water and possible boom failure. The confirmation of this needs a new dedicated experimental study. Available theoretical instability analyses, performed in this context, consider a steady inflow. Interesting works are, for instance, Leibovich (1976) and Smyth and Peltier (1989). The former examines the Kelvin-Helmoltz instability at the interfaces of three fluids (water, air and oil) and confirms, among others things, a greater instability for thicker oil. The latter examines possible transition between Kelvin-Helmoltz and Holmboe instabilities.

Oil leakage during boom failure When boom failure occurs oil is spelt downstream the boom, *i.e.* at its left side. The amount of this oil is an important parameter when dealing with real booms and their performances in waves and current. In this perspective, the present study is relevant in the case of slowly-varying currents or long waves since the flow inside

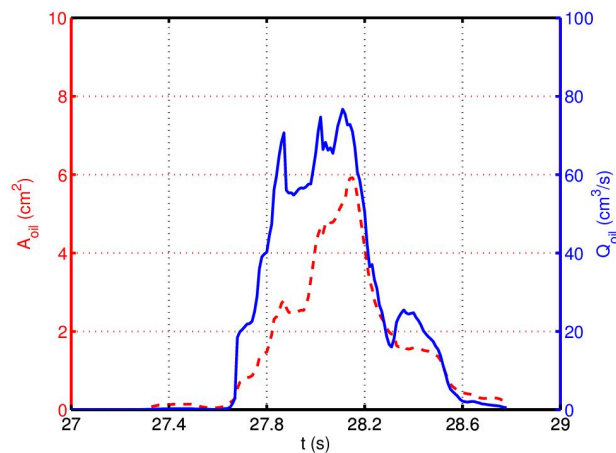
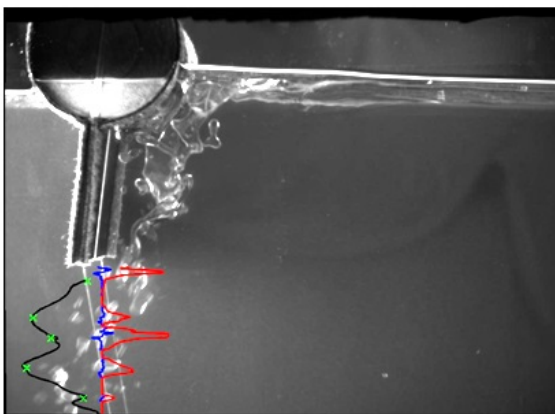


Figure 4: Left: snapshot from the image analysis used to estimate the average speeds and the cross-sectional circular areas of the oil along the selected vertical tank section. Right: time evolution of the total intersection area of the oil (A_{oil} , dashed line) and of the oil flux (Q_{oil} , solid line) for the case with $V_0 = 11$.

the tank is periodic with a long period. The volume of leaked oil is measured as time integral of the oil flux across a convenient vertical section of the tank near the mean position of the boom (see left plot of figure 4). At this stage the flow has clear 3D features. Therefore as a first approximation, for each oil droplet or filament passing the section, the corresponding intersection segment is assumed as the diameter of a corresponding circular oil cross-section. Left plot of figure 4 provides a snapshot exemplifying the performed analysis. The luminosity (red line) and its gradient (blue line) along the vertical tank section are used to identify and estimate the areas of the circular oil cross-sections. The PTV technique provides the horizontal speed (black line) along the section from which the averaged oil speed (indicated by a green cross) is evaluated for any intersection area. Using the averaged oil speeds and the cross-sectional areas, the oil flux (Q_{oil}) can be estimated in time. An example is provided in the right plot of figure 4 for the case with $V_0 = 1l$ (during the sixth period of tank motion), together with the evolution of the total intersection area of the oil (A_{oil}). These curves are obtained by smoothing the original data with a moving average filter that substitutes the instantaneous estimate of the variable with the average among the twenty estimates closest in time. This is done so to minimize the influence of errors associated with the identification process of the oil crossing the vertical section. From the results, both quantities (A_{oil} and Q_{oil}) change quickly in time because of the instability and breaking phenomena of the water-oil interface, leading to rapid passage of the oil below the boom. The boom failure starts around the time instant G of the examined period and lasts for this case about $0.24T$, with T the tank oscillation period. Reducing the initial volume V_0 leads to a delay in the boom failure and shortens the event duration. For example, with $V_0 = 0.9l$ the phenomenon lasts 30% less than with $V_0 = 1l$.

The time integration of the oil flux leads to the volume of oil leaked into the left side of the boom (V_l). Table 1 provides this quantity for all V_0 examined and shows a nonlinear behavior, with increasing slope toward largest V_0 and highest value of about 4% of V_0 for $V_0 = 1l$.

Table 1: Volume of leaked oil, V_l , for the different volumes of released oil, V_0 .

| | | | | | |
|-------------------|------|-----|------|------|-----|
| $V_0(ml)$ | 1000 | 900 | 800 | 700 | 500 |
| $V_l(ml)$ | 36.8 | 9.9 | 2.5 | 0.4 | 0 |
| $(V_l/V_0) * 100$ | 3.68 | 1.1 | 0.31 | 0.06 | 0 |

The physical investigation is still ongoing. From what discussed also above, some aspects highlighted the need for additional model tests. In particular, clearer views of the water-oil interface would help for a better understanding of the instability nature. It is also important to fully assess the relevance of the vortex shedding by reducing it through proper shaping of the boom and to investigate the instability occurrence in absence of the body. So a second-step experiment has been planned and the results from both activities will be documented at the Workshop.

This research activity is partially funded by the Research Council of Norway through the Centres of Excellence funding scheme AMOS, project number 223254, and partially by the Flagship Project RITMARE - The Italian Research for the Sea - coordinated by the Italian National Research Council and funded by the Italian Ministry of Education, University and Research within the National Research Program 2011-2013.

References

- DELVIGNE, G. (1989). Barrier failure by critical accumulation of viscous oil. In *International Oil Spill Conference Proceedings*, pp. 143–148.
- GRILLI, S., T. FAKE, AND M. SPAULDING (2000). Numerical Modeling of Oil Containment by a Boom/Barrier System : Phase III. Final Technical Report for DOT Grant. Technical Report DTRS57-95-G-00065, Dept. Ocean Engng., Univ. of Rhode Island.
- LEIBOVICH, S. (1976). Oil Slick Instability and the Entrainment Failure of Oil Containment Boom. *Journal of Fluids Engineering* 98, 98103.
- MIOZZI, M. (2004). Particle Image Velocimetry using Feature Tracking and Delaunay tessellation. In *12th Int. Symp. Applied Laser Techniques to Fluid Mechanics*, Lisbon, Portugal.
- SMYTH, W. D. AND W. R. PELTIER (1989). The Transition between KelvinHelmholtz and Holmboe Instability: An Investigation of the Overreflection Hypothesis. *J. Atmos. Sci.* 46, 36983720.